

University of Montana

## ScholarWorks at University of Montana

---

Chemistry and Biochemistry Faculty  
Publications

Chemistry and Biochemistry

---

8-11-2011

### The Nucleotide Exchange Factor Ric-8A is a Chaperone for the Conformationally Dynamic Nucleotide-Free State of G Alpha I1

Celestine J. Thomas

Klara Briknarova

Jonathan K. Hilmer

Navid Movahed

Brian Bothner

*See next page for additional authors*

Follow this and additional works at: [https://scholarworks.umt.edu/chem\\_pubs](https://scholarworks.umt.edu/chem_pubs)



Part of the [Biochemistry Commons](#), and the [Chemistry Commons](#)

## Let us know how access to this document benefits you.

---

#### Recommended Citation

Thomas, Celestine J.; Briknarova, Klara; Hilmer, Jonathan K.; Movahed, Navid; Bothner, Brian; Sumida, John P.; Tall, Gregory G.; and Sprang, Stephen R., "The Nucleotide Exchange Factor Ric-8A is a Chaperone for the Conformationally Dynamic Nucleotide-Free State of G Alpha I1" (2011). *Chemistry and Biochemistry Faculty Publications*. 32.

[https://scholarworks.umt.edu/chem\\_pubs/32](https://scholarworks.umt.edu/chem_pubs/32)

This Article is brought to you for free and open access by the Chemistry and Biochemistry at ScholarWorks at University of Montana. It has been accepted for inclusion in Chemistry and Biochemistry Faculty Publications by an authorized administrator of ScholarWorks at University of Montana. For more information, please contact [scholarworks@mso.umt.edu](mailto:scholarworks@mso.umt.edu).

---

**Authors**

Celestine J. Thomas, Klara Briknarova, Jonathan K. Hilmer, Navid Movahed, Brian Bothner, John P. Sumida, Gregory G. Tall, and Stephen R. Sprang

# The Nucleotide Exchange Factor Ric-8A Is a Chaperone for the Conformationally Dynamic Nucleotide-Free State of G $\alpha$ 1

Celestine J. Thomas<sup>1,2</sup>, Klára Briknarová<sup>1,3</sup>, Jonathan K. Hilmer<sup>4</sup>, Navid Movahed<sup>4</sup>, Brian Bothner<sup>4</sup>, John P. Sumida<sup>5</sup>, Gregory G. Tall<sup>6</sup>, Stephen R. Sprang<sup>1,2\*</sup>

**1** Center for Biomolecular Structure and Dynamics, The University of Montana, Missoula, Montana, United States of America, **2** Division of Biological Science, The University of Montana, Missoula, Montana, United States of America, **3** Department of Chemistry and Biochemistry, The University of Montana, Missoula, Montana, United States of America, **4** Proteomics and Mass Spectrometry Facility, Department of Chemistry and Biochemistry, Montana State University, Bozeman, Montana, United States of America, **5** Bioanalytical Pharmacy Core, University of Washington, Seattle, Washington, United States of America, **6** Department of Pharmacology and Physiology, School of Medicine and Dentistry, University of Rochester Medical Center, Rochester, New York, United States of America

## Abstract

Heterotrimeric G protein  $\alpha$  subunits are activated upon exchange of GDP for GTP at the nucleotide binding site of G $\alpha$ , catalyzed by guanine nucleotide exchange factors (GEFs). In addition to transmembrane G protein-coupled receptors (GPCRs), which act on G protein heterotrimers, members of the family cytosolic proteins typified by mammalian Ric-8A are GEFs for Gi/q/12/13-class G $\alpha$  subunits. Ric-8A binds to G $\alpha$ •GDP, resulting in the release of GDP. The Ric-8A complex with nucleotide-free G $\alpha$ 1 is stable, but dissociates upon binding of GTP to G $\alpha$ 1. To gain insight into the mechanism of Ric-8A-catalyzed GDP release from G $\alpha$ 1, experiments were conducted to characterize the physical state of nucleotide-free G $\alpha$ 1 (hereafter referred to as G $\alpha$ 1[ ]) in solution, both as a monomeric species, and in the complex with Ric-8A. We found that Ric-8A-bound, nucleotide-free G $\alpha$ 1 is more accessible to trypsinolysis than G $\alpha$ 1•GDP, but less so than G $\alpha$ 1[ ] alone. The TROSY-HSQC spectrum of [<sup>15</sup>N]G $\alpha$ 1[ ] bound to Ric-8A shows considerable loss of peak intensity relative to that of [<sup>15</sup>N]G $\alpha$ 1•GDP. Hydrogen-deuterium exchange in G $\alpha$ 1[ ] bound to Ric-8A is 1.5-fold more extensive than in G $\alpha$ 1•GDP. Differential scanning calorimetry shows that both Ric-8A and G $\alpha$ 1•GDP undergo cooperative, irreversible unfolding transitions at 47° and 52°, respectively, while nucleotide-free G $\alpha$ 1 shows a broad, weak transition near 35°. The unfolding transition for Ric-8A:G $\alpha$ 1[ ] is complex, with a broad transition that peaks at 50°, suggesting that both Ric-8A and G $\alpha$ 1[ ] are stabilized within the complex, relative to their respective free states. The C-terminus of G $\alpha$ 1 is shown to be a critical binding element for Ric-8A, as is also the case for GPCRs, suggesting that the two types of GEF might promote nucleotide exchange by similar mechanisms, by acting as chaperones for the unstable and dynamic nucleotide-free state of G $\alpha$ .

**Citation:** Thomas CJ, Briknarová K, Hilmer JK, Movahed N, Bothner B, et al. (2011) The Nucleotide Exchange Factor Ric-8A Is a Chaperone for the Conformationally Dynamic Nucleotide-Free State of G $\alpha$ 1. PLoS ONE 6(8): e23197. doi:10.1371/journal.pone.0023197

**Editor:** Bostjan Kobe, University of Queensland, Australia

**Received:** May 17, 2011; **Accepted:** July 7, 2011; **Published:** August 11, 2011

**Copyright:** © 2011 Thomas et al. This is an open-access article distributed under the terms of the Creative Commons Attribution License, which permits unrestricted use, distribution, and reproduction in any medium, provided the original author and source are credited.

**Funding:** This work was supported by the National Institutes of Health Grants DK46371 (to S.R.S.), RR16455, RR020185 and RR24237 (to B.B.), GM088242 to (G.G.T.), and The Murdock Charitable Trust (B.B.). Funding for Bioanalytical Pharmacy Core at the University of Washington's Center for the Intracellular Delivery of Biologics is provided by the Washington State Life Science Discovery Fund (grant number 2496490). The funders had no role in study design, data collection and analysis, decision to publish, or preparation of the manuscript.

**Competing Interests:** The authors have declared that no competing interests exist.

\* E-mail: Stephen.sprang@umontana.edu

## Introduction

As members of the Ras superfamily of regulatory GTP binding proteins, heterotrimeric G protein  $\alpha$  subunits (G $\alpha$ ) undergo cycles of activation and deactivation driven by binding and hydrolysis of GTP [1]. Conversion to the basal, inactive state results from the intrinsic GTP hydrolyase activity of the G protein. Reactivation is achieved by replacement of GDP by GTP at the nucleotide binding site, catalyzed by guanine nucleotide exchange factors (GEFs). Although the structural events that accompany GEF-catalyzed nucleotide exchange on small, Ras-like G proteins are relatively well understood [2], the mechanism of heterotrimeric G protein activation remains enigmatic. Agonist-activated, transmembrane G protein-coupled receptors (GPCRs) [3] are the best characterized heterotrimeric G protein GEFs. GPCRs act on plasma membrane-localized G protein heterotrimers that consist

of GDP-bound G $\alpha$  tightly associated with heterodimers of G $\beta$  and G $\gamma$  subunits. Recently, members of a family of predominantly cytosolic proteins, typified by mammalian Ric-8A, were identified as non-receptor GEFs that catalyze nucleotide exchange directly on G $\alpha$  subunits of the Gi/o/q/12/13 families [4]. Across phylogeny, Ric-8A paralogs act in GPCR-independent pathways to orient mitotic spindles in asymmetric cell division, as demonstrated in (*C. elegans* [5,6], *Drosophila* [7], and mammalian cells [8]).

Ric-8A is a soluble 59.7 kDa protein predicted to adopt a superhelical structure composed of  $\alpha$ -helical armadillo repeats [9]. In contrast to GPCRs, Ric-8A catalyzes the release of GDP directly on G $\alpha$  subunits, but has markedly weak affinity for G $\alpha$  bound to GTP or non-hydrolyzable GTP analogs [4]. Upon binding to G $\alpha$ 1•GDP, Ric-8A catalyzes GDP release and forms a stable nucleotide-free Ric-8A:G $\alpha$ 1[ ] complex (empty brackets:

“[ ]”, denote absence of bound nucleotide). In the presence of GTP, the complex dissociates to yield free Ric-8A and G $\alpha$ 1•GTP [4].

Using limited proteolysis, circular dichroism (CD) spectroscopy, heteronuclear NMR spectroscopy, hydrogen-deuterium exchange mass spectrometry (HD-MS), and differential scanning calorimetry (DSC), we have found that Ric-8A stabilizes G $\alpha$ 1 in a conformationally dynamic and heterogeneous state which, we propose, facilitates GDP release and subsequent GTP binding. We show that the C-terminus of G $\alpha$ 1 is a critical binding element for Ric-8A recognition and activity, as is also the case for GPCRs [10,11], suggesting that the two GEFs may act by convergent mechanisms.

## Results

### The smallest fragment of Ric-8A with full GEF activity encompasses most of the protein

We conducted limited trypsin proteolysis, together with mass spectroscopic and secondary structural analysis, to define a minimal fragment of Ric-8A that retained the activity of the full-length protein (Fig. 1A–C). The fragment encompassing residues 1–492 (Ric-8A $\Delta$ C492) exceeded full-length Ric-8A in GEF activity, whereas C-terminal truncations of successive predicted helical regions ( $\Delta$ C426,  $\Delta$ C453) or truncation of the N-terminus ( $\Delta$ N12,  $\Delta$ N38) in the background of  $\Delta$ C492 retained GDP release activity that was uncoupled from GTP $\gamma$ S binding stimulatory activity (Fig. 1D,E). Truncated proteins ( $\Delta$ C402,  $\Delta$ C374) bound G $\alpha$ 1•GDP weakly (data not shown) but had no nucleotide release or GEF activity. Because it is both more abundantly expressed in *Escherichia coli* and appears to biochemically more stable as well as more active than the full-length protein, we chose to conduct subsequent experiments with Ric-8A $\Delta$ C492. To enhance the sensitivity of tryptophan fluorescence assays of GEF activity, we used a non-myristoylated G $\alpha$ 1 mutant in which Trp 258 was substituted with alanine. The W258A mutation did not impair GTP binding, GTPase activity, or susceptibility to the GEF activity of Ric-8A (Fig. 2) [12]. For brevity, we refer to  $\Delta$ C492Ric-8A and W258AG $\alpha$ 1 as Ric-8A and G $\alpha$ 1, respectively.

### Relative to G $\alpha$ 1•GDP, nucleotide-free G $\alpha$ 1 is more accessible to protease digestion, and deficient in secondary structure

Trypsinolysis experiments demonstrated that G $\alpha$ 1[ ] was substantially more protease-sensitive than G $\alpha$ 1•GDP (Figures 3A and 3B) and was more rapidly degraded into <20 kDa fragments. The distribution of cleavage products is different in the free and GDP-bound states. Normalized as mean residue ellipticity, the CD spectrum of G $\alpha$ 1[ ] showed an overall reduction of regular secondary structure relative to G $\alpha$ 1•GDP (Figure 4). These results accord with earlier findings that G $\alpha$ 1[ ] is converted into a misfolded species with low affinity for guanine nucleotides [13]. G $\alpha$ 1[ ] bound to Ric-8A was more resistant to trypsinolysis than free G $\alpha$ 1[ ], as indicated by the persistence of fragments labeled 2 through 4 at the 10 minute time point in Figure 3E. Note, for example, that band 1, visible at the 5 minute time point of G $\alpha$ 1[ ], is degraded after 10 minutes of protease exposure (Figure 3B). The same fragment persisted after 10 minutes in the complex with Ric-8A (Figure 3E, band 3). Fragments 2–4 encompass the N-terminal residues of the Ras domain beyond the P-loop, together with most or all of the helical domain of G $\alpha$ 1 [14]. Nevertheless, Ric-8A-bound G $\alpha$ 1[ ] was still more susceptible to proteolysis than G $\alpha$ 1•GDP (Figure 3A). In contrast, if bound to G $\alpha$ 1, Ric-8A was more sensitive to protease digestion than free Ric-8A (Figures 3D

and 3E). After 10 minutes of protease digestion of Ric-8A:G $\alpha$ 1[ ], all Ric-8A fragments with molecular weights greater than ~24 kDa were degraded, yet several fragments of greater length remained intact after free Ric-8A was exposed to trypsin for the same duration. For both free and G $\alpha$ 1-bound Ric-8A, residues 141–348 appears to constitute a relatively protease-resistant protein core (bands 3 and 1 in Figure 3D and 3E, respectively; for reference to the predicted secondary structure of Ric-8A see Figure 1C). Note that no protease inhibitors were present in the trypsin preparation used to generate the data shown in Figure 3, so the extent of Ric-8A degradation is greater than that shown in Figure 1A.

The mass-normalized CD spectra of Ric-8A and Ric-8A:G $\alpha$ 1[ ] show similar degrees of secondary structure formation. Therefore, we infer that Ric-8A-bound G $\alpha$ 1[ ] possesses higher secondary structure content than free G $\alpha$ 1[ ]. Both spectra are indicative of predominantly  $\alpha$ -helical structure, whereas G $\alpha$ 1•GDP shows evidence of both  $\alpha$ -helical and  $\alpha$ -sheet structure, which is characteristic of the Ras-like domain of this and other G proteins [1] (Figure 4). The near absence of  $\beta$ -sheet structure estimated from the CD spectrum of Ric-8A:G $\alpha$ 1[ ] suggests that changes in secondary structure may occur in the  $\alpha/\beta$  Ras-like domain of G $\alpha$ 1 upon binding to Ric-8A and subsequent release of GDP.

### Peaks in the $^{15}\text{N}$ - $^1\text{H}$ HSQC spectrum of G $\alpha$ 1 are severely attenuated upon binding to Ric-8A

To elucidate the structural properties of G $\alpha$ 1 bound either to nucleotides or to Ric-8A, we acquired  $^1\text{H}$ - $^{15}\text{N}$  Transverse Relaxation Optimized (TROSY) Heteronuclear Single Quantum Coherence (HSQC) spectra [15] of [ $^{15}\text{N}$ ]G $\alpha$ 1. The  $^1\text{H}$ - $^{15}\text{N}$  TROSY-HSQC spectrum of G $\alpha$ 1•GDP (Figure 5A) and G $\alpha$ 1•GTP $\gamma$ S (data not shown) showed ~300 moderately well resolved and dispersed peaks, comparable in quality to spectra reported by Abdulaev, *et al.* [16] for a GDP-bound chimera (G $\alpha$ t/i) of transducin  $\alpha$  (G $\alpha$ t) and G $\alpha$ 1. In contrast, the spectrum of [ $^{15}\text{N}$ ]G $\alpha$ 1:Ric-8A showed considerable diminution in the amplitude of many peaks, indicative of extensive line broadening (Figure 5B). Significant changes in chemical shift were not observed upon binding to Ric-8A. Gel filtration of the sample after data collection confirmed that Ric-8A:[ $^{15}\text{N}$ ]G $\alpha$ 1[ ] remained a homogeneous heterodimer over the time-scale of the NMR experiment, and did not aggregate (data not shown). Peak broadening observed in the spectrum of Ric-8A:[ $^{15}\text{N}$ ]G $\alpha$ 1[ ] could result from exchange among conformational states of Ric-8A-bound G $\alpha$ 1[ ] in the intermediate  $\mu$ s-ms time scale, and/or from slow tumbling of the 96 kDa complex. Subsequent re-acquisition of the  $^1\text{H}$ - $^{15}\text{N}$  TROSY-HSQC spectrum after addition of GTP $\gamma$ S to dissociate the complex and removal of free Ric-8A, afforded a [ $^{15}\text{N}$ ]G $\alpha$ 1•GTP $\gamma$ S spectrum identical to that of G $\alpha$ 1•GTP $\gamma$ S prepared in the absence of Ric-8A (Figure 5C), thus demonstrating that G $\alpha$ 1 bound to Ric-8A in the NMR sample retained biochemical activity.

### The population of rapidly exchanging G $\alpha$ 1 protons doubles upon Ric-8A binding and release of GDP

To test the hypothesis that Ric-8A-bound G $\alpha$ 1[ ] adopts a state of high conformational flexibility, we conducted HD-MS exchange experiments [17] to directly assess changes in structural dynamics of G $\alpha$ 1 upon formation of the Ric-8A:G $\alpha$ 1[ ] complex. Hydrogen-deuterium exchange in either G $\alpha$ 1•GDP or Ric-8A:G $\alpha$ 1[ ] was initiated by rapid dilution of the proteins into D $_2$ O buffer. To determine the rate and extent of HD exchange,

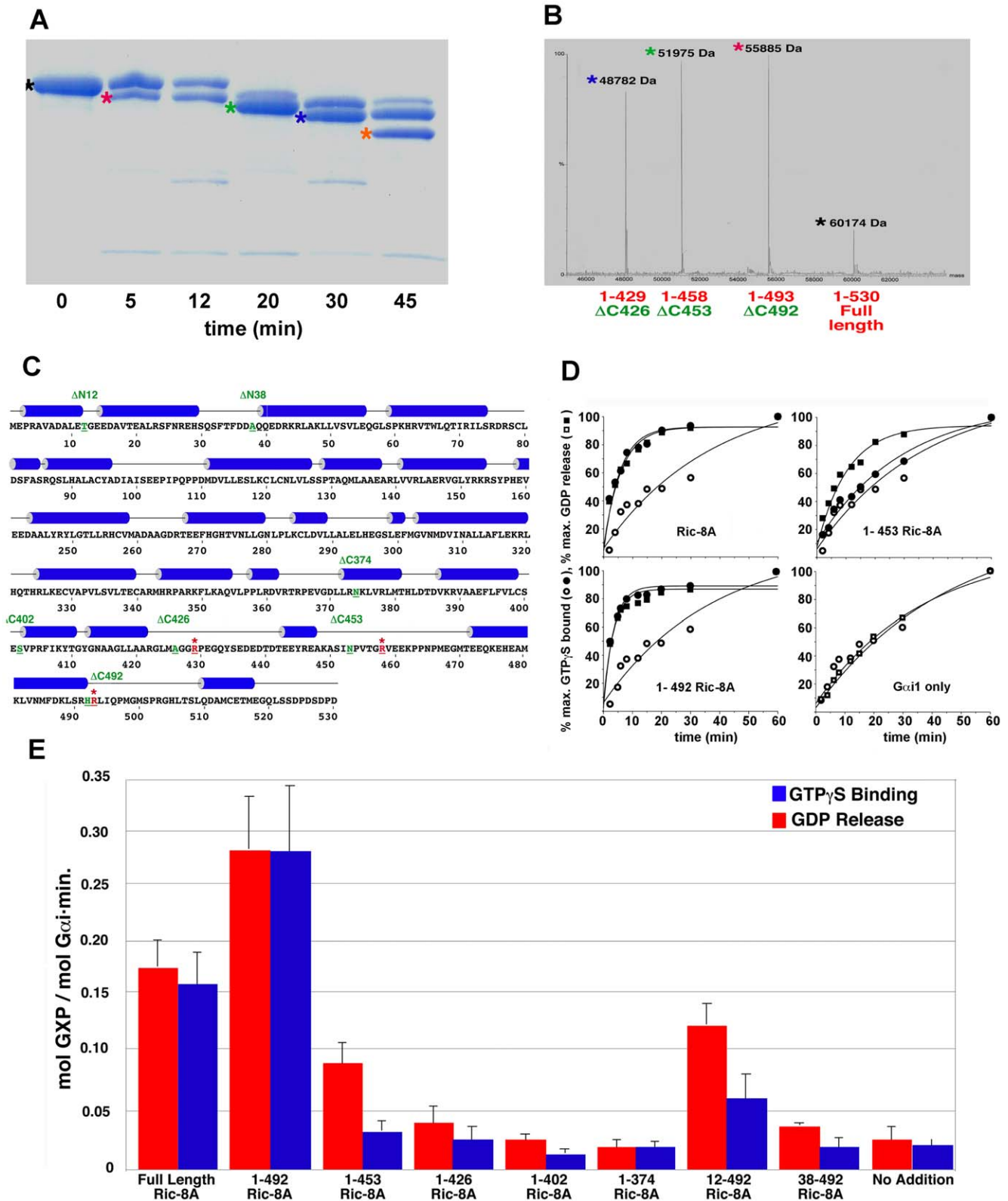


**Figure 1. GEF activity of purified Ric-8A fragments defined by limited trypsinolysis and secondary structure analysis.** (A) Coomassie-stained SDS PAGE analysis of Ric-8A after trypsinolysis for the times indicated below each lane; unique fragments are identified by colored asterisks. (B) Electrospray mass spectrometric analysis of Ric-8A tryptic digest fragments extracted from the SDS PAGE gel shown in panel A; peaks identified by asterisks refer to corresponding bands shown in panel A. Fragment masses (Da) are indicated at each peak position. (C) Amino acid sequence of rat Ric-8A; cylinders indicate helical segments predicted using JPRED [51]. Residue codes colored red indicate sites of proteolytic cleavage (see panel A). Residue codes in green indicate N or C-termini of recombinant Ric-8A fragments engineered to coincide approximately with proteolytic sites or predicted secondary structure boundaries: ΔC492 denotes the Ric-8A fragment comprising residues 1–492. Both N-terminal truncations ΔN12 and

ΔN38 were also C-terminally truncated at residue 492 and comprised residues 12–492 and 38–492, respectively. (D) Kinetics of intrinsic (open symbols) or Ric-8A-stimulated (filled symbols) GDP release (squares) from, or GTPγ binding to (circles) myristoylated Gαi1 were determined by a filter binding assay using radiolabeled nucleotides as described [4]. Upper left panel, Gαi1 (200 nM) nucleotide binding and release in the presence of full-length Ric-8A (200 nM); lower left panel, ΔC492Ric-8A (200 nM); upper right panel, ΔC453Ric-8A (200 nM); lower right panel, Gαi1 alone. Data for each panel are normalized to maximum GDP released or GTPγ bound in a single experiment. Data points represent the average of three experiments; standard deviation from the mean is <10%. Time course of GTPγ binding in the absence of Ric-8A, shown at lower right, is replicated in the other panels for comparison. (E), Histogram showing relative rates of Gαi1 GDP release (red bars) and GTPγ binding (blue bars) catalyzed by Ric-8A and Ric-8A truncation mutants (200 nM). Error bars represent ± one standard deviation of the apparent first-order rate constants determined in three replicates.  
doi:10.1371/journal.pone.0023197.g001

the exchange reaction was quenched with formic acid/acetonitrile at successive time intervals, and the products analyzed by electrospray mass spectrometry (ES-MS). For each time-point, the mass distribution of Gαi1 was determined by deconvolution of the raw m/z spectrum (Figure 6A,B). The mass distribution of Gαi1•GDP remained unimodal throughout the 60 minute exchange period (Figure 6A), whereas that for Gαi1[] bound to Ric-8A evolved into a multimodal distribution, suggestive of conformational heterogeneity (Figure 6B). Analysis of these data revealed a nearly four-fold greater initial rate of deuterium exchange in Ric-8A-bound Gαi1[] than in Gαi1•GDP (Figure 6C). After 60 minutes of exposure to D<sub>2</sub>O, the mass of Gαi1[] in the complex with Ric-8A increased by ~340 Da, accounting for more than half of all the exchangeable Gαi1 protons, versus a ~210 Da mass increase in Gαi1•GDP alone. The enhanced rate and extent of deuterium substitution is indicative of greater solvent accessibility at exchangeable sites in Ric-8A-bound Gαi1 than in Gαi1•GDP, most likely due to amplified breathing motions in the Ric-8A:Gαi1[] complex [18].

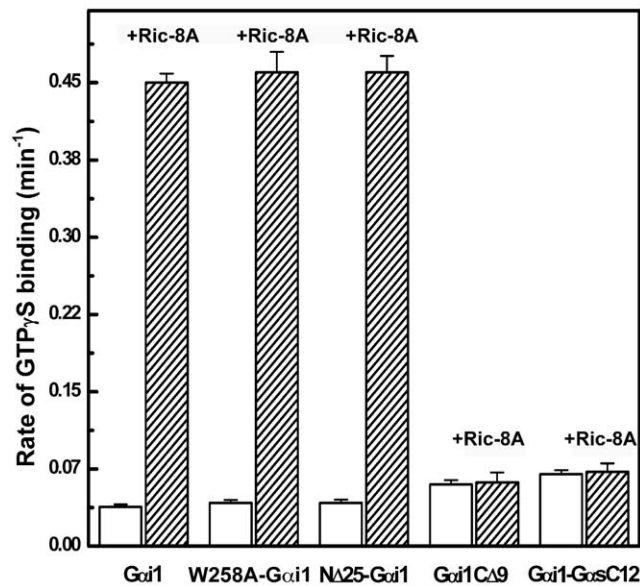


**Figure 2. Intrinsic and Ric-8A-catalyzed GTPγS binding rates of the Gαi1 proteins used in this study.** Intrinsic and Ric-8A-catalyzed kinetics of binding of GTPγS to wild-type Gαi1, W258A-Gαi1, NΔ25Gαi1, Gαi1CΔ9 and Gαi1-GαsC12 were measured using a fluorescence binding assay [12,47]. 400 μl of protein (1 μM) in the GDP bound form was equilibrated for 10–15 min at 25°C in a cuvette. A 10-fold excess of GTPγS was added and fluorescence at 340 nm upon excitation at 290 nm was monitored in the absence (open bars) or presence (filled bars) of Ric-8A (1 μM). Error bars represent ± one standard deviation apparent first-order rate constants determined in three replicates.  
doi:10.1371/journal.pone.0023197.g002

### Thermodynamic stability of both nucleotide-free Gαi1 and Ric-8A increase upon complex formation

We used differential scanning calorimetry (DSC), by which change in heat capacity (C<sub>p</sub>) is measured as a function of

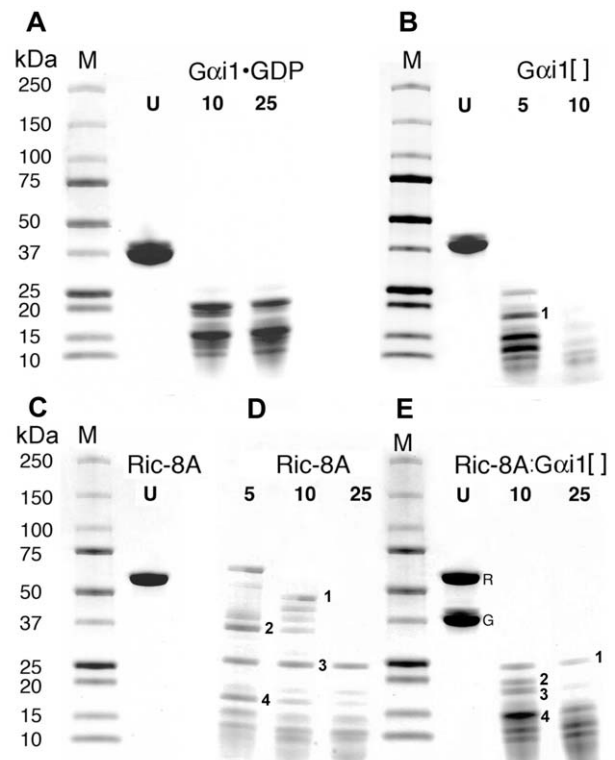


**Figure 3. Ric-8A provides limited protection of nucleotide-free Gαi1 from trypsin digestion.** Samples were incubated with TPCK treated trypsin at a 1:1000 molar ratio (trypsin:sample) at 4°C, withdrawn at the indicated time points, separated by SDS-PAGE and visualized by Coomassie blue staining. (A) Gαi1•GDP: lanes from left to right: molecular weight markers, M; untreated Gαi1•GDP, U; samples digested for 10 and 25 minutes. (B) nucleotide-free Gαi1[]: markers, M; untreated Gαi1[], U; samples digested for 5 and 10 minutes. Mass spectroscopic analysis identifies band 1 as Gαi1 residues 21–179: observed/calculated mass 17,761/17,774 Da. (C) Ric-8A: markers, M; untreated, U. (D) Ric-8A: after 5, 10 and 15 minutes of trypsin digestion. Mass analysis identifies band 1 as Ric-8A residues 1–408: 46,218/46,207 Da; band 2, residues 72–378: 34,815/34,799; band 3, residues 141–348: 23,834/23,804 Da; band 4, residues 62–178: 13,563/13,523 Da. (E) Ric-8A: Gαi1[] complex; markers, M; untreated Ric-8A:Gαi1[] complex; R and G indicate bands for intact Ric-8A and Gαi1, respectively; Ric-8A:Gαi1[] complex digested for 10 and 25 minutes. Mass analysis identifies band 1 as Ric-8A residues 141–348: 23,834/23,804 Da (present also as band 3 in Panel D); band 2, Gαi1 residues 17–191: 19,646/19,652 Da; band 3, Gαi1 residues 21–179: 17,753/17,761 Da (present as band 1 in panel B); band 4: Gαi1 residues 10–141: 14,532/14,520 Da.  
doi:10.1371/journal.pone.0023197.g003

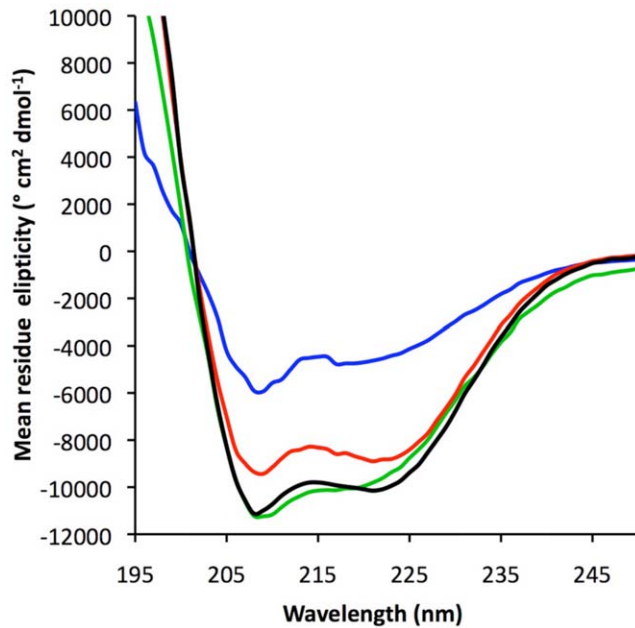


**Figure 4. Nucleotide-free Gαi1 is relatively unstructured in comparison to Gαi1•GDP, but regains helical secondary structure in the complex with Ric-8A.** Circular dichroic spectra were normalized as mean residue ellipticity, and predicted secondary structure assignments are: Ric-8A, red: 87%  $\alpha$ -helix; Ric-8A:Gαi1[ ], black: 87%  $\alpha$ -helix, 0.5%  $\beta$ -strand; Gαi1•GDP, green: 51%  $\alpha$ -helix, and 11%  $\beta$ -strand; Gαi1[ ], blue, 38%  $\alpha$ -helix, 9%  $\beta$ -strand.  
doi:10.1371/journal.pone.0023197.g004

temperature, to determine the modality and mid-point temperatures ( $T_m$ ) for the unfolding transitions of Gαi1•GDP, Gαi1[ ], Ric-8A and Ric-8A:Gαi1[ ] [19]. At temperatures below and above the thermal unfolding transition of a protein, the  $C_p$  exhibits a linear,

typically positive, dependence on the temperature of the native and unfolded states, respectively. In the region of the thermal transition,  $C_p$  exceeds that of both the denatured and native states as hydrophobic groups are increasingly exposed to the aqueous solvent, and reaches a maximum value at  $T_m$  [20,21,22].

Gαi1•GDP underwent an irreversible cooperative unfolding transition with  $T_m = 52^\circ\text{C}$  (Figure 7, blue trace). The irreversible nature of the transition of this and the other proteins and protein complexes reported here precludes accurate determination of the enthalpy of unfolding, but allows comparison of the significant thermal features of the four species when measured at equivalent scan rates. Only a weak transition near  $33^\circ\text{C}$  was observed for Gαi1[ ] (Figure 7, dashed blue trace), which exhibited changes in  $C_p$  that were close to the detection limits of the instrument. The nucleotide-free protein thus appears to be conformationally heterogeneous or disordered [23], consistent with its high protease sensitivity (Figure 3B) and CD spectrum (Figure 4). Ric-8A itself underwent an irreversible cooperative folding transition with  $T_m = 47^\circ\text{C}$  (Figure 7, black trace). Thermal denaturation of Ric-8A:Gαi1[ ] was characterized by a nearly linear increase in heat capacity, suggestive of non-cooperative unfolding, followed by a discrete cooperative transition at  $50^\circ\text{C}$  (Figure 7, green trace), higher than the melting temperature of free Ric-8A. This latter  $T_m$  is invariant with protein concentration (data not shown), indicating that the complex remains intact throughout the transition. The denaturation profile of Ric-8A:Gαi1[ ] complex cannot be modeled as weighted average of the profiles of Ric-8A and Gαi1[ ] (Figure 7, red dashed line), hence the complex has unique thermodynamic properties relative to Gαi1[ ] and Ric-8A.

#### The C-terminus of Gαi1 is a specific and critical recognition element for Ric-8A binding and GEF activity

The mechanism by which Ric-8A catalyzes nucleotide exchange is similar in some respects to the analogous reaction catalyzed by GPCR at G $\beta\gamma$ -bound G $\alpha$  subunits. Experimental evidence

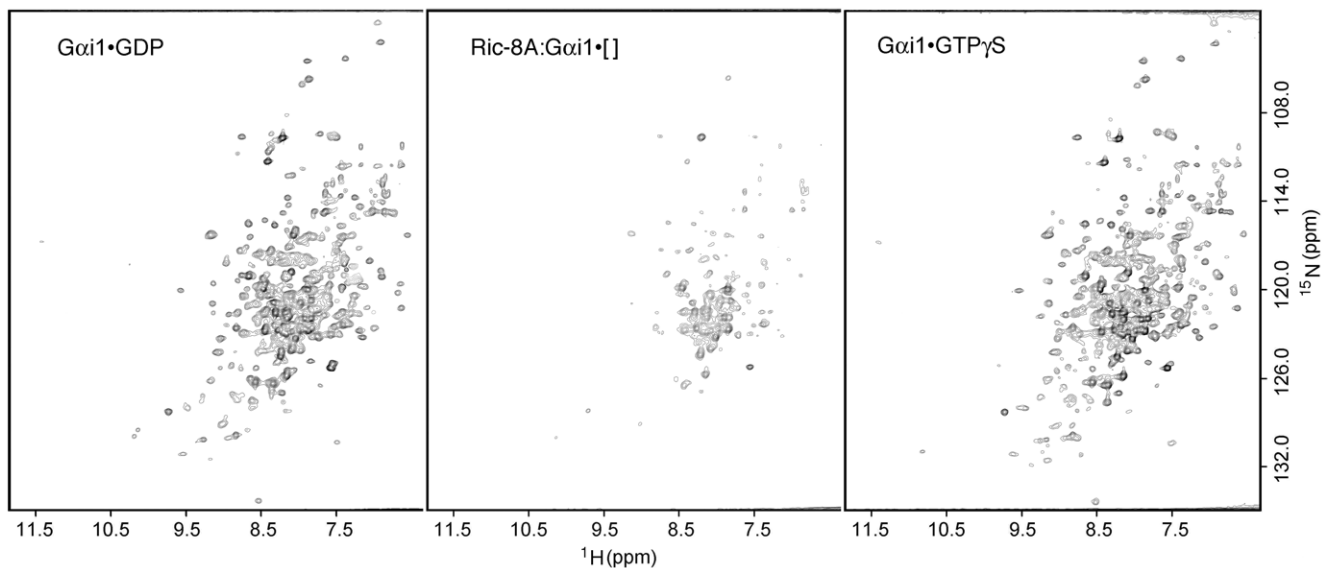


**Figure 5.  $^1\text{H}$ - $^{15}\text{N}$  TROSY-HSQC spectrum of Gαi1 shows extensive peak broadening and intensity loss upon binding of Ric-8A.** (A)  $^1\text{H}$ - $^{15}\text{N}$  HSQC-TROSY spectra were acquired for [ $^{15}\text{N}$ ]Gαi1•GDP, and (B) Ric8A:[ $^{15}\text{N}$ ]Gαi1[ ]. (C) After acquisition of the Ric-8A:[ $^{15}\text{N}$ ]Gαi1[ ] spectrum, a five molar excess of GTP $\gamma$ S was added to induce dissociation of Ric-8A and formation of Gαi1•GTP $\gamma$ S. After a short incubation, the free Ric-8A was removed by adsorption to IMAC resin and the  $^1\text{H}$ - $^{15}\text{N}$  TROSY-HSQC spectrum of the sample was recorded. Protein concentration, acquisition and processing parameters and contour levels in all panels are the same.  
doi:10.1371/journal.pone.0023197.g005

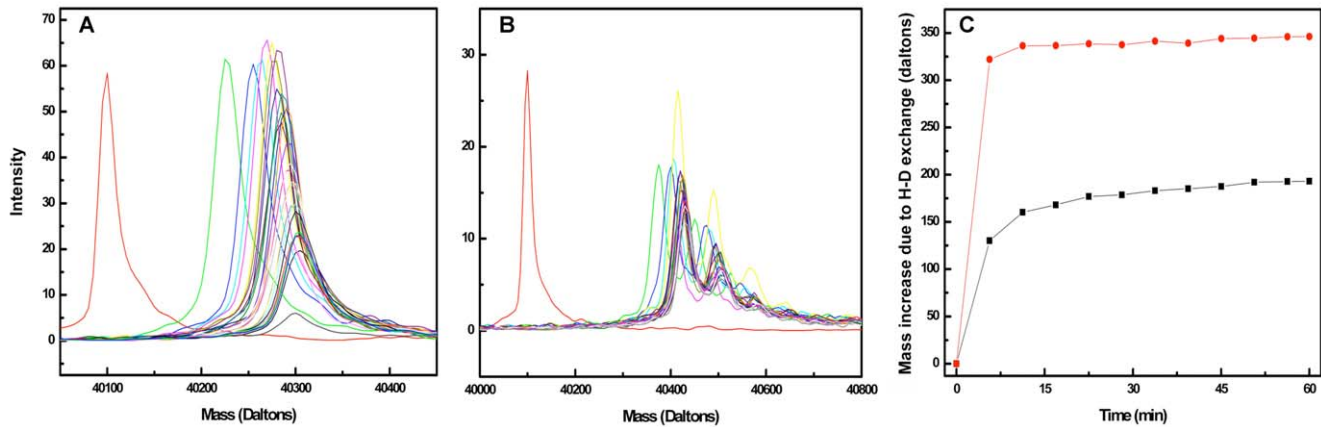


**Figure 6. Nucleotide-free G*α*1 bound to Ric-8A exhibits rapid hydrogen/deuterium exchange kinetics relative to the G*α*1•GDP complex.** (A) Mass distribution for G*α*1•GDP measured at fixed time points (see panel C) after dilution into D<sub>2</sub>O; the mass distribution at the zero time point, before exchange was initiated, corresponds to the red peak centered at 40.1 kDa. The average of the G*α*1 mass distribution increases as H/D exchange reaction proceeds. (B) Mass distribution for G*α*1[] in complex with Ric-8A measured at fixed time points after dilution into D<sub>2</sub>O; note that the G*α*1[] mass distribution becomes multimodal as the H/D exchange reaction proceeds. (C) The increase in mass (Da), determined at the centroid of the mass distribution of G*α*1•GDP (black squares) and G*α*1[] derived from the complex with Ric-8A (red circles) is plotted as a function of time after rapid dilution from aqueous buffer into D<sub>2</sub>O.  
doi:10.1371/journal.pone.0023197.g006

indicates that specific recognition and binding of the C-terminus of G*α* is crucial to the action of Ric-8A, just as it is for GPCRs [10,11]. First, a yeast two-hybrid screen of a rat brain library using a bait construct comprising Ric-8A residues 1–297 yielded a prey clone expressing the C-terminal 81 residues of G*α*1, that also interacted with a full-length Ric-8A bait construct (Figure 8A). Second, the peptide G*α*1C18, which is composed of a sequence of amino acid residues identical to that of the 18 C-terminal residues of G*α*1, inhibited Ric-8A-catalyzed exchange of GTPγS for GDP with an IC<sub>50</sub> of 23 μM (Figure 8B). Isothermal calorimetric

measurements indicated that G*α*1C18 binds directly to Ric-8A with a K<sub>d</sub> of 12 μM (Figure 8C). Third, G*α*1CΔ9, a G*α*1 truncation mutant lacking the nine C-terminal residues of the native protein, fails to serve as a substrate for Ric-8A although it retains GTP binding and hydrolytic activity [24] (Figure 2). Finally, substitution of the C-terminal twelve residues of G*α*1 with the corresponding residues of G*α*s, a G*α* protein that does not bind to Ric-8A [4], abrogated susceptibility to the GEF activity of Ric-8A (Figure 2) but did not impair GTP binding activity. These results are in accord with recent findings that pertussis toxin-

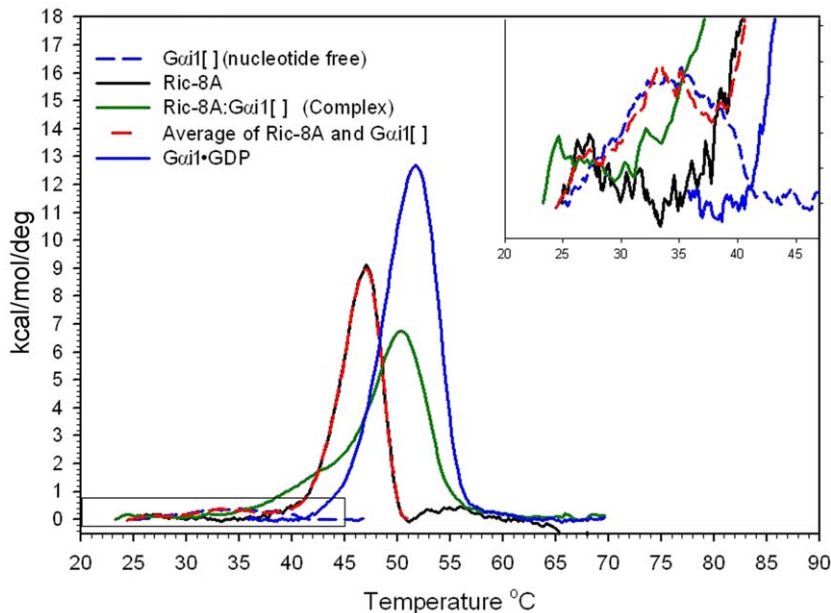


**Figure 7. Thermal denaturation properties of G*α*1 and Ric-8A are affected by their mutual interaction.** Temperature-dependence of heat capacity was measured by differential scanning calorimetry. Buffer baseline-corrected thermograms were recorded for Ric-8A (black trace), G*α*1 [] (dashed blue trace), G*α*1•GDP (blue trace) and Ric-8A:G*α*1[] (green trace). The weighted average of the thermograms for Ric-8A and G*α*1[] (red dashed line) overlaps that of G*α*1[] in the temperature range below ~37°C and that of Ric-8A above that temperature, and is distinct from the thermogram of Ric-8A:G*α*1[]. The inset shows a magnified view of the four thermograms and the weighted average function in the 20°C–45°C range.  
doi:10.1371/journal.pone.0023197.g007



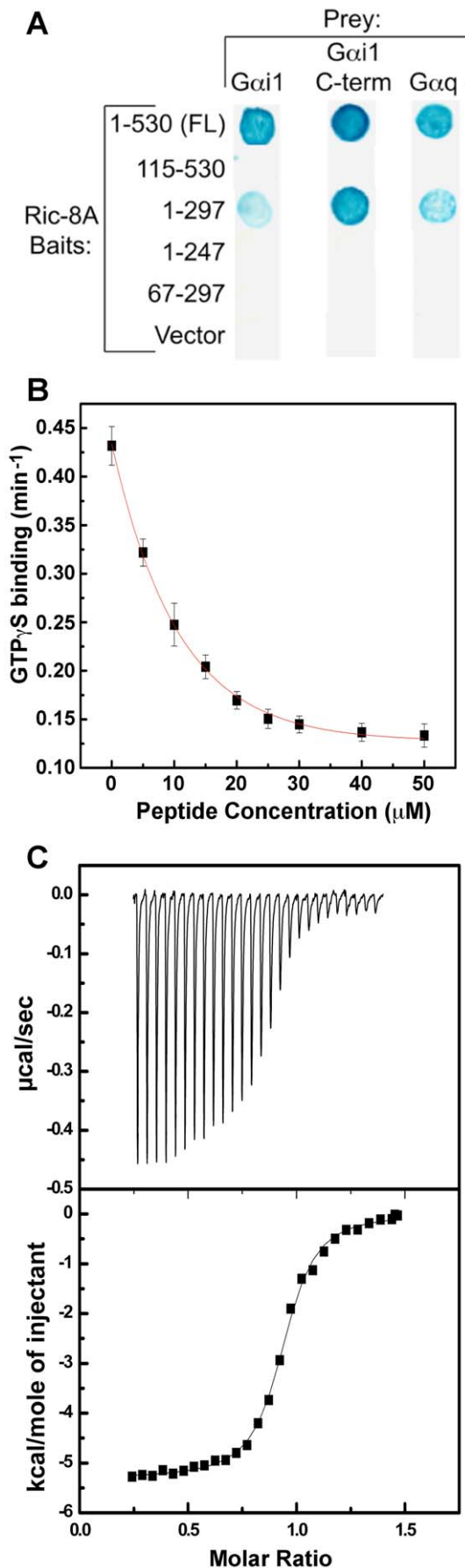


**Figure 8. The carboxyl-terminus of Gαi1 interacts with the amino-terminus of Ric-8A.** (A) Yeast two-hybrid screen; prey clones encoding full-length Gαi1, Gαq and the carboxyl-terminal 81 amino acids of Gαi1 were tested pair-wise using a  $\beta$ -galactosidase filter assay for interactions with the full-length Ric-8A bait (amino acids, 1–530 FL), and truncated Ric-8A bait constructs (amino acids: 115–530, 1–297, 1–247, 67–297), and the empty prey vector. (B) Inhibition by Gαi1C18, a peptide composed of the 18 C-terminal residues of Gαi1, on Ric-8A-catalyzed binding of GTP $\gamma$ S to Gαi1 was assayed by fluorescence emission from an endogenous Gαi1 tryptophan. To 1  $\mu$ M Gαi1•GDP in the presence of 1  $\mu$ M Ric-8A, pre-incubated with different concentrations of Gαi1C18, was added a 10-fold excess of GTP $\gamma$ S and fluorescence at 340 nm upon excitation at 290 nm was monitored. GTP $\gamma$ S binding rates, obtained by fitting the time-dependent rise in fluorescence, plotted as a function of peptide concentration, yields an  $IC_{50}$  of 23  $\mu$ M for Gαi1C18 inhibition of Ric-8A nucleotide exchange activity. Data points shown are the mean, and error bars indicate the standard deviation, for three separate determinations. (C) Isothermal titration calorimetric determination of binding of Gαi1C18 to Ric-8A. Peptide (250  $\mu$ M) was injected into a calorimeter cell containing 25  $\mu$ M Ric-8A. The top panel shows the baseline corrected isotherm and the bottom panel indicates the fit of the same performed with a single binding site model, yielding a dissociation constant of 12  $\mu$ M for binding of Gαi1C18 to Ric-8A at 25°C. The calculated enthalpy for the reaction was  $-5.3$  kcal/mol with a stoichiometry (N) of 0.9. doi:10.1371/journal.pone.0023197.g008

catalyzed ADP ribosylation at the C-terminus of Gαi1 [8] and that truncation of the twelve Gαi1 C-terminal residues [25] blocks Ric-8A binding and GEF activity. On the other hand, truncation of 25 residues from the N-terminus of Gαi1 did not affect its susceptibility to the GEF activity of Ric-8A (Figure 2).

## Discussion

The experiments described in this report provide insight into the mechanism of Ric-8A-catalyzed exchange of GDP for GTP on Gαi1. In this reaction, Ric-8A:Gαi1 [ ] is a stable intermediate that does not readily dissociate in the absence of GTP or non-hydrolysable GTP analogs. We have shown that, within this complex, Gαi1 [ ] adopts a considerably more dynamic conformation than nucleotide-bound Gαi1, but is more structured and less susceptible to proteolysis than free Gαi1 [ ]. This is in sharp contrast to most nucleotide-free complexes of small G proteins with cognate GEFs, in which both the GEF and G protein components are typically well ordered structures [2].

Ric-8A-catalyzed nucleotide exchange proceeds through a stable (in the absence of GTP) but loosely structured intermediate. Examples of enzymes that stabilize proteins in unfolded or disordered states include chaperones such as GroEL [26], and AAA+ ATPase unfoldases of ClpXP proteases and related proteases that degrade mis-folded proteins [27]. However, Ric-8A functions differently from these, in that it is not coupled to an exergonic reaction (*e.g.* ATPase activity), but does exhibit high substrate specificity and catalyzes a discrete chemical transformation. We propose that the catalytic power of Ric-8A derives, in part, from its ability to act (in rough analogy with GroEL and other unfoldases) as a chaperone for a partially unfolded or disordered conformation Gαi1 [ ], thereby reducing the activation energy barrier to GDP release and GTP binding, while disfavoring unproductive side reactions that would lead to Gαi1 deactivation and aggregation. In the partially unstructured state induced and stabilized by Ric-8A, the nucleotide binding site of Gαi1 may be more solvent-accessible than in the nucleotide-bound state.

The mechanism by which Ric-8A catalyzes nucleotide exchange may be similar in some respects to the analogous reaction catalyzed by GPCR at G $\beta\gamma$ -bound G $\alpha$  subunits. Recognition and

binding of the G $\alpha$  C-terminus is crucial to the action of both exchange factors. In a manner analogous to that proposed for GPCRs, Ric-8A could promote nucleotide release by gripping, and perhaps tensioning, the C-terminus of G $\alpha$  and thereby weaken local tertiary structure ( $\alpha$ 5 helix,  $\beta$ 5 and  $\beta$ 6 strands) that is allosterically coupled to the purine binding site and switch regions [11,28,29]. Indeed, the substantial reduction in fluorescence emission of Trp 211 in switch II of G $\alpha$ 1 upon binding to Ric-8A provides evidence for such perturbations [12]. Whether Ric-8A directly engages the switch regions of G $\alpha$  is uncertain. Such interactions might be precluded since Ric-8A is able to form a transient ternary complex with G $\alpha$ 1•GDP:AGS3 [12]. AGS3, a guanine nucleotide dissociation inhibitor, comprises GPR/Go-Loco motifs [30,31] that partially block the switch I/switch II interface [32]. Similarly, direct interactions between GPCRs and the switch regions of G $\alpha$  are problematic on stereochemical grounds [33]. It is also noteworthy in this context that importin- $\beta$ , a protein involved in the transport of protein cargo into the nucleus, and also a presumptive structural analog of Ric-8A, has been shown to act as a GEF for Ran1•GDP [34]. Crystallographic analysis demonstrates that importin- $\beta$  induces conformational changes in the switch regions of Ran1•GDP [35].

Both GPCRs and Ric-8A appear to induce or maintain a dynamic state of G $\alpha$ . NMR studies of complexes between [ $^{15}$ N]G $\alpha$ 1/t: $\beta$ 1 $\gamma$ 1 and rhodopsin mimetics show that resonances in the G $\alpha$  subunit are highly broadened [36], as we have observed for Ric-8A: G $\alpha$ 1 [ ]. In contrast, the HSQC spectrum of [ $^{15}$ N]G $\alpha$ 1/t bound to G $\beta$ 1 $\gamma$ 1, a complex with a molecular mass comparable to Ric-8A: [ $^{15}$ N]G $\alpha$ 1 [ ], is well defined and similar to that of G $\alpha$ 1/t•GDP [37]. Recent evidence obtained from double electron resonance (DEER) spectroscopy shows that, in the activated rhodopsin-heterotrimer complex, nucleotide-free G $\alpha$ 1 is conformationally heterogeneous, and that the Ras-like and helical domains of G $\alpha$ 1, between which nucleotide is bound, swing away from each other [38]. The NMR and HD-MS data presented here suggest that nucleotide-free G $\alpha$ 1 bound to Ric-8A undergoes conformational exchange, with interconversion times that are possibly in the  $\mu$ s-ms range. The DSC melting profile of Ric-8A:G $\alpha$ 1 [ ] is suggestive of a non-cooperative unfolding transition at lower temperature followed by a discrete transition near 50°C. It seems reasonable to attribute the former to a conformationally heterogeneous and dynamic G $\alpha$ 1 [ ] and the latter to Ric-8A, which in the complex with G $\alpha$ 1 [ ] is more thermostable yet also more protease accessible than unbound Ric-8A, suggesting that Ric-8A itself may undergo some structural change upon binding to G $\alpha$ 1. However, structural assignment of transitions in the DSC spectra is speculative. It remains to be determined which segments of G $\alpha$ 1 become mobile within the nucleotide free complex with Ric-8A, and importantly, to confirm that induction or stabilization of a partially disordered or conformationally flexible state in G $\alpha$ 1 in fact reduces the kinetic energy barrier to GDP release and GTP binding.

## Materials and Methods

### Molecular Cloning and Protein Expression

The open reading frame of rat Ric-8A and truncation variants (encompassing residues 1–492, 12–492, 1–453, 1–426, 1–402, 1–374, 12–492 and 38–492) were amplified by PCR and subcloned into the pET-28a vector for expression as N-terminally hexahistidine tagged proteins. Proteins were expressed in *Escherichia coli* BL21 (DE3)-RIPL cells in LB media containing ampicillin (120 mg/L) and induced with 300  $\mu$ M isopropyl  $\beta$ -D-thiogalactopyranoside (IPTG) at 20°C. After overnight growth at 20°C, cells

were lysed by sonication at 20°C in lysis buffer (50 mM Tris, pH 8.0, 250 mM NaCl, 2 mM DTT, and 2 mM PMSF). The cell lysate was clarified by centrifugation and loaded onto a column containing 5 ml of nickel NTA-agarose (GE Healthcare). After extensive washing with lysis buffer, proteins were eluted from the resin with buffer (50 mM Tris, pH 8.0, 150 mM NaCl and 2 mM PMSF) containing 250 mM imidazole and dialyzed in a low ionic strength buffer (50 mM Tris, pH 8.0, 2 mM DTT, and 2 mM PMSF). The dialysate was loaded onto a UNO-Q matrix (Bio-Rad) and eluted with a 0–500 mM NaCl gradient on an AKTA FPLC system (GE Healthcare). Pure Ric-8A $\Delta$ C492 eluted from the matrix at 165–175 mM NaCl.

Rat G $\alpha$ 1 was expressed as a tobacco etch virus protease (TEV)-cleavable, N-terminal glutathione-S-transferase (GST) fusion protein as described [12]. W258A-G $\alpha$ 1, in which the tryptophan residue at position 258 is substituted by alanine, was generated by use of the QuikChange (Stratagene) kit according to the manufacturer's protocol, using the pDEST-15 vector harboring wild type GST-G $\alpha$ 1 as a template. To generate  $\Delta$ 25-G $\alpha$ 1, from which the N-terminal 25 residues of the native protein are deleted, attB-modified primers corresponding to amino acids 25 to 35 and 343 to 353 of G $\alpha$ 1 were used for PCR amplification and cloning of the fragment into the pDEST15 vector. W258A-G $\alpha$ 1 and  $\Delta$ 25-G $\alpha$ 1 were expressed and purified as described [12].

The plasmid pBN905, which expresses rat G $\alpha$ 1 $\Delta$ C9, lacking the C-terminal nine residues of the native protein, fused in-frame to intein-CBD cDNA in the pTXB3 expression vector (New England Biolabs), was a kind gift from Dr. T.J. Baranski, Washington University, St. Louis, MO. G $\alpha$ 1 $\Delta$ C9 was expressed and purified as described [39]. With the exception of experiments summarized in Figure 1, 2 and 8A, all other experiments were performed with Ric-8A $\Delta$ C492 and W258A-G $\alpha$ 1, which we henceforth refer to as Ric-8A and G $\alpha$ 1, respectively.

Nucleotide-free G $\alpha$ 1 proteins were prepared by the method of Ferguson and Higashijima [40], using exchange and dialysis buffers composed of 50 mM Tris.HCl, pH 8.1, 2 mM Tris (2-carboxyethyl)phosphene (TCEP) with 20% glycerol (v/v) and 150 mM NaCl. GTP $\gamma$ S-bound G $\alpha$ 1 was prepared as described [41].

### Preparation of $^{15}$ N-labeled proteins

[ $^{15}$ N]G $\alpha$ 1 was prepared as described with minor modifications [42]. Briefly, transformed *E. coli* cells were grown in minimal media supplemented with [ $^{15}$ N]NH $_4$ Cl (Cambridge Isotopes, 99.8% purity) and [ $^{15}$ N]Bioexpress Cell Growth media (10 ml of 10 $\times$  concentrate/liter of media) (Cambridge Isotope Labs), induced with 500  $\mu$ M IPTG at 20°C and allowed to express G $\alpha$ 1 overnight at the same temperature. The purification protocol was identical to that used for native proteins and the yields were approximately one third lower.

### Preparation of Ric-8A:G $\alpha$ 1 complexes

Nucleotide-free Ric-8A:G $\alpha$ 1 and Ric-8A:[ $^{15}$ N]G $\alpha$ 1 complexes were generated by incubating equimolar concentrations of Ric-8A (500  $\mu$ l of 150  $\mu$ M protein) with G $\alpha$ 1•GDP or [ $^{15}$ N]G $\alpha$ 1 (500  $\mu$ l of 150  $\mu$ M protein) overnight in sample buffer (20 mM Tris•HCl, pH 8.0, 150 mM NaCl, 2 mM DTT, and 5 mM EDTA) containing 50  $\mu$ l of immobilized alkaline phosphatase (Sigma) to hydrolyze released nucleotide, and gently rocked at 4°C. The immobilized alkaline phosphatase was removed by centrifugation, and complex was gel-filtered over tandem Superdex 200/75 gel filtration columns pre-equilibrated in 20 mM Tris, pH 8.0, 150 mM NaCl, 2 mM DTT and eluted at a flow rate of 0.4 ml/min using an AKTA FPLC (GE Healthcare).

### Trypsin Protection Assays

To samples containing Ric-8A, G $\alpha$ i1•GDP, G $\alpha$ i1[ ] or Ric-8A:G $\alpha$ i1 (50  $\mu$ M in 50 mM Tris-HCl, pH 8.0, 150 mM NaCl and 2 mM DTT), L-1-*p*-tosylamido-2-phenylethyl chloromethyl ketone (TPCK)-treated trypsin (Sigma) was added at a molar ratio of 1000:1. Samples were incubated at 4°C for 5, 10, 15 and 25 minutes. For each time point, a 10  $\mu$ l aliquot was withdrawn, diluted in SDS-PAGE loading buffer, boiled, separated by SDS-PAGE and visualized by Coomassie staining. Proteolytic products were eluted from the gel slices and subjected to MALDI-TOF mass spectrometry on a Voyager DE3 (Applied Biosystems) or by electrospray mass spectrometry using on a Agilent 6520 QTOF. Limited trypsinolysis for mass spectrometric identification of large Ric-8A fragments (Figure 1) was conducted in the presence of a 1:2 molar ratio of bovine pancreatic aprotinin to TPCK-trypsin. Proteolytic products were eluted from the gel slices and subjected to electrospray mass spectrometry and N-terminal sequencing at the Protein Chemistry Core Facility of the University of Texas Southwestern Medical Center.

### Yeast two hybrid experiments

A rat brain yeast two-hybrid prey library [43] was screened with a pVJL11 [44] bait construct encoding the amino-terminal 297 amino acids of Ric-8A (1–297) in the L40 yeast strain [45] with a prey clone consisting of the carboxyl-terminal 81 amino acids of G $\alpha$ i1 (G $\alpha$ i1 C-term). Full-length G $\alpha$ i1 and G $\alpha$ q, and the G $\alpha$ i1 C-term preys, in pGADGH (Clontech) were then tested pair-wise using a  $\beta$ -galactosidase filter assay for interactions with the full-length Ric-8A bait (amino acids, 1–530 FL), and truncated Ric-8A bait constructs that coded for different regions of the Ric-8A protein (amino acids: 115–530, 1–297, 1–247, 67–297), or the empty prey vector.

### [<sup>35</sup>S]GTP $\gamma$ S Binding Assays

Binding of [<sup>35</sup>S]GTP $\gamma$ S to wild-type G $\alpha$ i1 or W258A-G $\alpha$ i1, in the presence or absence of Ric-8A was performed using a filter binding method [46] in a 50 mM Tris-HCl, pH 8.0, 150 mM NaCl, 2 mM DTT and 0.05% polyoxyethylene lauryl ether (C12E10).

### Pull-down assays for G $\alpha$ i1 binding to Ric-8A fragments

Equimolar amounts of Ric-8A and G $\alpha$ i1 (10  $\mu$ M protein in 50 mM TRIS. HCl, pH 8.0, 150 mM NaCl, 2 mM DTT and 0.05% C12E10) were incubated overnight at 4°C. 10  $\mu$ l of a 50% slurry of Ni<sup>+2</sup> IMAC (BioRad) resin was then added to the mixture, incubated for one hour, washed thrice with 500  $\mu$ l of wash buffer (50 mM Tris, pH 8.0, 250 mM NaCl, 1 mM DTT and 2 mM PMSF) and the proteins retained on the beads were visualized by Coomassie stained SDS-PAGE.

### Peptide synthesis

An amidated peptide, G $\alpha$ i1C18, corresponding to the C-terminal 18 residues of rat G $\alpha$ i1 (DAVTDVVIKNNLKDCGLF) was synthesized using standard Fmoc chemistry by the Protein Chemistry Core laboratory at UT Southwestern Medical Center at Dallas and purified to near homogeneity by HPLC (Agilent Technologies) on a pre-packed C18 matrix (Waters). Mass of the peptide was confirmed by MALDI-TOF mass spectrometry (Voyager DE, Applied Biosystems).

### Peptide competition assays

Exchange of GTP $\gamma$ S for GDP bound to G $\alpha$ i1 or G $\alpha$ i1C $\Delta$ 9 was followed by monitoring the change in the tryptophan fluorescence

of G $\alpha$ i1, as described [12]. G $\alpha$ i1•GDP (1  $\mu$ M) in 20 mM HEPES, pH 8.0, 100 mM NaCl, 10 mM MgCl<sub>2</sub>, 1 mM DTT, and 0.05% C12E10 in a reaction volume of 400  $\mu$ l was allowed to equilibrate for 10–15 min at 20°C in a quartz fluorescence cuvette. GTP $\gamma$ S (final concentration, 10  $\mu$ M) was added to the reaction mixture in the absence or presence of 1  $\mu$ M Ric-8A, and the increase in fluorescence at 340 nm was monitored upon excitation at 290 nm [47]. Exchange kinetics were also measured in the presence of 1  $\mu$ M Ric-8A and (5–50  $\mu$ M) G $\alpha$ i1C18. Protein and peptide mixtures were preincubated for one hour before addition of GTP $\gamma$ S. Fluorescence measurements were conducted using an LS55 spectrofluorometer (PerkinElmer Life Sciences) attached to a circulating water bath to maintain a steady sample temperature of 20°C. Excitation and emission slit widths were set at 2.5 nm. All exciting light was eliminated by use of a 290 nm cut-off filter positioned in front of the emission photomultiplier.

### Circular Dichroism spectroscopy

G $\alpha$ i1•GDP, Ric-8A, G $\alpha$ i1[ ] or the nucleotide free binary complex of the two proteins at 4  $\mu$ M each in 25 mM HEPES, pH 7.2, 150 mM NaCl and 2 mM DTT and, in the case of G $\alpha$ i1[ ], 20% v/v glycerol, were dispensed into a 300- $\mu$ l quartz cuvette with a 1 mm path length. CD spectra in the range of 195–245 nm were measured at a scan rate of 1 nm/min using a PiStar-180 CD spectrometer (Applied Photophysics). The scans were repeated thrice; the data were averaged and the CD spectra of the buffer was subtracted. The optical path and the cuvette chamber were continually flushed with a nitrogen flow throughout the course of the experiment. Secondary structure analysis was performed using K2D2 [48].

### NMR spectroscopy

Protein samples for NMR spectroscopy ([<sup>15</sup>N]G $\alpha$ i1•GDP, [<sup>15</sup>N]G $\alpha$ i1:Ric-8A or [<sup>15</sup>N]G $\alpha$ i1•GTP $\gamma$ S) were dialyzed against 20 mM sodium phosphate, pH 6.8, 75 mM NaCl and 2 mM DTT in 10% <sup>2</sup>H<sub>2</sub>O/90% H<sub>2</sub>O, and concentrated to 250  $\mu$ M. The [<sup>15</sup>N]G $\alpha$ i1•GTP $\gamma$ S sample was prepared from the [<sup>15</sup>N]G $\alpha$ i1:Ric-8A complex by addition of five molar excess of GTP $\gamma$ S and incubation for 10 minutes at 25°C. Free Ric-8A, and non-dissociated [<sup>15</sup>N]G $\alpha$ i1:Ric-8A complex were then removed with Ni<sup>+2</sup> IMAC resin (BioRad). <sup>1</sup>H-<sup>15</sup>N TROSY-HSQC spectra [49] were acquired at 25°C on a 600 MHz Varian NMR System equipped with a salt-tolerant cold probe and processed with Felix 2004 (Felix NMR, Inc.).

### Hydrogen-Deuterium Exchange Mass Spectrometry

Hydrogen-deuterium exchange of the G $\alpha$ i1•GDP or Ric-8A:G $\alpha$ i1[ ] was analyzed by automated reverse-phase HPLC coupled to electrospray ionization TOF mass spectrometry. The HPLC consisted of an Agilent 1100 HPLC with a G1377a autosampler, and the ESI-TOF was a Bruker microTOF. Following initiation of the reaction by ten-fold dilution of protein stock (1 mg/ml G $\alpha$ i1•GDP or Ric-8A:G $\alpha$ i1[ ], in 20 mM sodium phosphate, pH 6.8, 100 mM NaCl and 1 mM DTT) into D<sub>2</sub>O, the reaction mixture was pipetted into a sealed autosampler vial and the autosampler was used to draw aliquots at regular time intervals. Quenching of the exchange reaction was achieved by rapid binding of the protein onto a C4 reverse phase cartridge from Michrom Bioresources (8×1 mm) and subsequent washing and elution. The column and autosampler were pre-equilibrated with 20% (v/v) acetonitrile, 80% H<sub>2</sub>O and 0.1% formic acid (w/v), pH 2.2, prior to sample loading. Immediately following sample (0.5  $\mu$ l) injection, the solvent composition was changed to 100% acetonitrile, 0.1% formic acid. By using a rapid step gradient and

very high flow rates of 600  $\mu$ l/min, the sample was minimally delayed in the flow path to the mass spectrometer, eluting at approximately 0.4 minutes. The column system was equilibrated at 4°C to minimize back-exchange. Data processing was performed with the Bruker Data Analysis software package, version 4.0. The Maximum Entropy deconvolution routine was used to perform charge-deconvolution for the spectral range of 700 m/z to 1400 m/z, which encompassed the majority of the observed distribution of protein signal. The deconvoluted spectra were exported to ORIGIN software and the centroid masses for G $\alpha$ 1 were calculated and plotted as a function of time.

### Differential Scanning Calorimetry (DSC)

For DSC analysis, G $\alpha$ 1•GDP, Ric-8A and Ric-8A:G $\alpha$ 1 [ ] were dialyzed against degassed DSC sample buffer: 25 mM PIPES pH 7.2, 150 mM NaCl and 1 mM TCEP, and additionally for the G $\alpha$ 1•GDP sample, 20  $\mu$ M GDP. DSC buffer for G $\alpha$ 1 [ ] contained 20% glycerol (v/v). Immediately before DSC analysis, protein samples were clarified by centrifugation at 14,000 RPM for 10 min in a bench-top Eppendorf microfuge. Protein concentrations after dilution, if required, were determined by least squares fitting of predicted protein extinction coefficients to spectra in the 220–420 nm range measured on a HP diode array instrument. The measured values were 3.6  $\mu$ M for G $\alpha$ 1•GDP, 5.9  $\mu$ M for Ric-8A, 5.1  $\mu$ M for Ric-8:G $\alpha$ 1 [ ] and 7.9  $\mu$ M for G $\alpha$ 1 [ ]. DSC measurements were conducted using a Microcal capDSC with autosampler (MicroCal, GE Healthcare). After establishing a thermal history by running water vs. water scans, three buffer against water scans were conducted for each sample using the corresponding dialysate solution to obtain the buffer Cp over the experimental temperature range. Following this, two buffer vs protein scans were performed. Protein samples were rescanned once to check for thermal reversibility.

A typical thermal cycle involved cooling the instrument to 20°C after which a 10 min. thermal equilibration was initiated. Following thermal equilibration, scanning of the sample was performed at a scan rate of 1°C/min over a 20°C–70°C range

using passive feedback gain mode and a filtering period of 5 seconds. Once the experimental high temperature limit was reached (70°C), the instrument was cooled back to the starting temperature.

Data analysis was performed using Origin 7.0 by first subtracting the last buffer scan from the protein thermal scan. After normalizing the data to the protein concentration, a progressive baseline estimation was performed by calculating the fractional contribution of the native and denatured state to the sample Cp at each point beneath the excess heat capacity function, thus producing a smoothly varying function of temperature [50]. Data presented in Figure 7 were corrected by subtraction of the temperature-dependent change in Cp of the buffer. A weighted average thermal profile for G $\alpha$ 1 [ ] and Ric-8A was computed using the expression  $C_p^{Av}(T) = w^{Ric-8A} C_p^{Ric-8A}(T) + w^{G\alpha 1[ ]} C_p^{G\alpha 1[ ]}(T)$ , where  $w^{Ric-8A}$  and  $w^{G\alpha 1[ ]}$  are weighting factors for Ric-8A and G $\alpha$ 1 [ ] contributions to the heat capacity at temperature T, and  $C_p^{Ric-8A}$  and  $C_p^{G\alpha 1[ ]}$  are the heat capacities measured for free Ric-8A and G $\alpha$ 1 [ ] at that temperature.

### Acknowledgments

We thank Kevin Gardner for demonstrating feasibility of HSQC experiments, Jessica Glicken for assistance with [<sup>15</sup>N] isotopic enrichment, Bruce Bowler and members of his laboratory for discussions regarding CD experiments and assistance with CD data collection, Brian Crammer at the Genomics Proteomics core facility of the Rocky Mountain Regional Center of Excellence at Colorado State University for assistance with electrospray mass spectrometric analysis, William Atkins for directing us to the Bioanalytical Pharmacy Core resources at the University of Washington, and Elizabeth Goldsmith for critical reading of early versions of the manuscript.

### Author Contributions

Conceived and designed the experiments: SRS CJT JPS BB KB JH GGT. Performed the experiments: CJT JPS KB NM JH GGT. Analyzed the data: SRS KB CJT JPS JH GGT. Contributed reagents/materials/analysis tools: KB JPS JH BB. Wrote the paper: SRS CJT JPS JH.

### References

1. Sprang SR (1997) G protein mechanisms: Insights from structural analysis. *Annu Rev Biochem* 66: 639–678.
2. Cherfils J, Chardin P (1999) GEFs: structural basis for their activation of small GTP-binding proteins. *Trends Biochem Sci* 24: 306–311.
3. Pierce KL, Premont RT, Lefkowitz RJ (2002) Seven-transmembrane receptors. *Nat Rev Mol Cell Biol* 3: 639–650.
4. Tall GG, Krumins AM, Gilman AG (2003) Mammalian Ric-8A (synembryn) is a heterotrimeric G $\alpha$  protein guanine nucleotide exchange factor. *J Biol Chem* 278: 8356–8362.
5. Afshar K, Willard FS, Colombo K, Johnston CA, McCudden CR, et al. (2004) RIC-8 Is Required for GPR-1/2-Dependent G $\alpha$  Function during Asymmetric Division of *C. elegans* Embryos. *Cell* 119: 219–230.
6. Müller KG, Emerson MD, McManus JR, Rand JB (2000) RIC-8 (Synembryn): a novel conserved protein that is required for G(q) signaling in the *C. elegans* nervous system. *Neuron* 27: 289–299.
7. David NB, Martin CA, Segalen M, Rosenfeld F, Schweisguth F, et al. (2005) Drosophila Ric-8 regulates Galphai cortical localization to promote Galphai-dependent planar orientation of the mitotic spindle during asymmetric cell division. *Nat Cell Biol* 7: 1083–1090.
8. Woodard GE, Huang NN, Cho H, Miki T, Tall GG, et al. Ric-8A and G $\alpha$ 1 recruit LGN, NuMA, and dynein to the cell cortex to help orient the mitotic spindle. *Mol Cell Biol* 30: 3519–3530.
9. Figueroa M, Hinrichs MV, Bunster M, Babbitt P, Martínez-Oyanedel J, et al. (2009) Biophysical studies support a predicted superhelical structure with armadillo repeats for Ric-8. *Protein Sci* 18: 1139–1145.
10. Oldham WM, Hamm HE (2008) Heterotrimeric G protein activation by G-protein-coupled receptors. *Nat Rev Mol Cell Biol* 9: 60–71.
11. Scheerer P, Park JH, Hildebrand PW, Kim YJ, Krauss N, et al. (2008) Crystal structure of opsin in its G-protein-interacting conformation. *Nature* 455: 497–502.
12. Thomas CJ, Tall GG, Adhikari A, Sprang SR (2008) Ric-8A catalyzes guanine nucleotide exchange on G $\alpha$ 1 bound to the GPR/GoLoco exchange inhibitor AGS3. *J Biol Chem* 283: 23150–23160.
13. Zelen B, Veklich Y, Murray J, Parkes JH, Gibson S, et al. (2001) Rapid irreversible G protein alpha subunit misfolding due to intramolecular kinetic bottleneck that precedes Mg<sup>2+</sup> “lock” after GTP/GDP exchange. *Biochemistry* 40: 9647–9656.
14. Coleman DE, Berghuis AM, Lee E, Linder ME, Gilman AG, et al. (1994) Structures of active conformations of G $\alpha$ 1 and the mechanism of GTP hydrolysis. *Science* 265: 1405–1412.
15. Pervushin K, Riek R, Wider G, Wüthrich K (1997) Attenuated T<sub>2</sub> relaxation by mutual cancellation of dipole-dipole coupling and chemical shift anisotropy indicates an avenue to NMR structures of very large biological macromolecules in solution. *Proceedings of the National Academy of Sciences of the United States of America* 94: 12366–12371.
16. Abdulaev NG, Zhang C, Dinh A, Ngo T, Bryan PN, et al. (2005) Bacterial expression and one-step purification of an isotope-labeled heterotrimeric G-protein alpha-subunit. *J Biomol NMR* 32: 31–40.
17. Hoofnagle AN, Resing KA, Ahn NG (2003) Protein analysis by hydrogen exchange mass spectrometry. *Annu Rev Biophys Biomol Struct* 32: 1–25.
18. Englander SW, Downer NW, Teitelbaum H (1972) Hydrogen exchange. *Annual Review of Biochemistry* 41: 903–924.
19. Privalov PL, Potekhin SA (1986) Scanning microcalorimetry in studying temperature-induced changes in proteins. *Methods in Enzymology* 131: 4–51.
20. Privalov PL, Khechinashvili NN (1974) A thermodynamic approach to the problem of stabilization of globular protein structure: A calorimetric study. *J Mol Biol* 86: 665–684.
21. Privalov PL, Gill SJ (1988) Stability of protein structure and hydrophobic interaction. *Advances in Protein Chemistry* 39: 191–234.
22. Prabhu NV, Sharp KA (2005) Heat capacity in proteins. *Annu Rev Phys Chem* 56: 521–548.
23. Griko YV, Privalov PL (1994) Thermodynamic puzzle of apomyoglobin unfolding. *J Mol Biol* 235: 1318–1325.
24. Anderson LL, Marshall GR, Baranski TJ (2005) Expressed protein ligation to study protein interactions: semi-synthesis of the G-protein alpha subunit. *Protein Pept Lett* 12: 783–787.

25. Vellano CP, Shu FJ, Ramineni S, Yates CK, Tall GG, et al. (2011) Activation of the regulator of G protein signaling 14-Gα<sub>i</sub>1-GDP signaling complex is regulated by resistance to inhibitors of cholinesterase-8A. *Biochemistry* 50: 752–762.
26. Horwich AL, Apetri AC, Fenton WA (2009) The GroEL/GroES cis cavity as a passive anti-aggregation device. *FEBS Lett* 583: 2654–2662.
27. Sauer RT, Bolon DN, Burton BM, Burton RE, Flynn JM, et al. (2004) Sculpting the proteome with AAA(+) proteases and disassembly machines. *Cell* 119: 9–18.
28. Oldham WM, Van Eps N, Preininger AM, Hubbell WL, Hamm HE (2007) Mapping allosteric connections from the receptor to the nucleotide-binding pocket of heterotrimeric G proteins. *Proc Natl Acad Sci U S A* 104: 7927–7932.
29. Kapoor N, Menon ST, Chauhan R, Sachdev P, Sakmar TP (2009) Structural evidence for a sequential release mechanism for activation of heterotrimeric G proteins. *J Mol Biol* 393: 882–897.
30. Peterson YK, Bernard ML, Ma H, Hazard S, 3rd, Graber SG, et al. (2000) Stabilization of the GDP-bound conformation of G<sub>α</sub> by a peptide derived from the G-protein regulatory motif of AGS3. *J Biol Chem* 275: 33193–33196.
31. Siderovski DP, Diverse-Pierluissi M, De Vries L (1999) The GoLoco motif: a Gα<sub>i</sub>/o binding motif and potential guanine- nucleotide exchange factor. *Trends Biochem Sci* 24: 340–341.
32. Kimple RJ, Kimple ME, Betts L, Sondek J, Siderovski DP (2002) Structural determinants for GoLoco-induced inhibition of nucleotide release by Gα<sub>i</sub> subunits. *Nature* 416: 878–881.
33. Oldham WM, Van Eps N, Preininger AM, Hubbell WL, Hamm HE (2006) Mechanism of the receptor-catalyzed activation of heterotrimeric G proteins. *Nat Struct Mol Biol* 13: 772–777.
34. Lonhienne TG, Forwood JK, Marfori M, Robin G, Kobe B, et al. (2009) Importin-β is a GDP-to-GTP exchange factor of Ran: implications for the mechanism of nuclear import. *J Biol Chem* 284: 22549–22558.
35. Forwood JK, Lonhienne TG, Marfori M, Robin G, Meng W, et al. (2008) Kap95p binding induces the switch loops of RanGDP to adopt the GTP-bound conformation: implications for nuclear import complex assembly dynamics. *J Mol Biol* 383: 772–782.
36. Abdulaev NG, Ngo T, Ramon E, Brabazon DM, Marino JP, et al. (2006) The receptor-bound “empty pocket” state of the heterotrimeric G-protein α-subunit is conformationally dynamic. *Biochemistry* 45: 12986–12997.
37. Abdulaev NG, Ngo T, Zhang C, Dinh A, Brabazon DM, et al. (2005) Heterotrimeric G-protein α-subunit adopts a “preactivated” conformation when associated with βγ-subunits. *J Biol Chem* 280: 38071–38080.
38. Van Eps N, Preininger AM, Alexander N, Kaya AI, Meier S, et al. (2011) Interaction of a G protein with an activated receptor opens the interdomain interface in the α subunit. *Proc Natl Acad Sci U S A* 108: 9420–9424.
39. Anderson LL, Marshall GR, Crocker E, Smith SO, Baranski TJ (2005) Motion of carboxyl terminus of Gα<sub>i</sub> is restricted upon G protein activation. A solution NMR study using semisynthetic Gα<sub>i</sub> subunits. *J Biol Chem* 280: 31019–31026.
40. Ferguson KM, Higashijima T (1991) Preparation of guanine nucleotide-free G proteins. *Methods Enzymol* 195: 188–192.
41. Coleman DE, Lee E, Mixon MB, Linder ME, Berghuis A, et al. (1994) Crystallization and preliminary crystallographic studies of G<sub>αi1</sub> and mutants of G<sub>αi1</sub> in the GTP and GDP-bound states. *J Mol Biol* 238: 630–634.
42. Holdeman TC, Gardner KH (2001) <sup>1</sup>H, <sup>13</sup>C and <sup>15</sup>N chemical shift assignments of the N-terminal PAS domain of mNPAS2. *J Biomol NMR* 21: 383–384.
43. Sugita S, Hata Y, Südhof TC (1996) Distinct Ca<sup>2+</sup>-dependent properties of the first and second C<sub>2</sub>-domains of synaptotagmin I. *J Biol Chem* 271: 1262–1265.
44. Vojtek AB, Hollenberg SM, Cooper JA (1993) Mammalian Ras interacts directly with the serine/threonine kinase Raf. *Cell* 74: 205–214.
45. Fabian JR, Vojtek AB, Cooper JA, Morrison DK (1994) A single amino acid change in Raf-1 inhibits Ras binding and alters Raf-1 function. *Proceedings of the National Academy of Sciences USA* 91: 5982–5986.
46. Sternweis P, Robishaw J (1984) Isolation of two proteins with high affinity for guanine nucleotides from membranes of bovine brain. *J Biol Chem* 259: 13806–13813.
47. Higashijima T, Ferguson KM (1991) Tryptophan fluorescence of G proteins: analysis of guanine nucleotide binding and hydrolysis. *Methods in Enzymology* 195: 321–328.
48. Perez-Iratxeta C, Andrade-Navarro MA (2008) K2D2: estimation of protein secondary structure from circular dichroism spectra. *BMC Structural Biology* 8: 25.
49. Weigelt J (1998) Single Scan, Sensitivity- and Gradient-Enhanced TROSY for Multidimensional NMR Experiments. *J Am Chem Soc* 120: 10778–10779.
50. Cooper, Nutley, Wadwood (2000) *Differential Scanning Microcalorimetry*; Harding SE, Chowdry BZ, eds. Oxford, New York: Oxford University Press.
51. Cole C, Barber JD, Barton GJ (2008) The Jpred 3 secondary structure prediction server. *Nucleic Acids Res.* pp w197–201.